

Computational inverse design for ultra-compact single-piece metalenses free of chromatic and angular aberration

Cite as: Appl. Phys. Lett. **118**, 041104 (2021); doi: [10.1063/5.0035419](https://doi.org/10.1063/5.0035419)

Submitted: 1 November 2020 · Accepted: 6 January 2021 ·

Published Online: 27 January 2021



View Online



Export Citation



CrossMark

Zin Lin,^{1,a)} Charles Roques-Carmes,² Rasmus E. Christiansen,^{3,b)} Marin Soljačić,^{4,c)} and Steven C. Johnson¹

AFFILIATIONS

¹Department of Mathematics, Massachusetts Institute of Technology, Cambridge, Massachusetts 02138, USA

²Research Lab of Electronics, Massachusetts Institute of Technology, Cambridge, Massachusetts 02138, USA

³Department of Mechanical Engineering, Technical University of Denmark, Nils Koppels Allé, Building 404, 2800 Kongens Lyngby, Denmark

⁴Department of Physics, Massachusetts Institute of Technology, Cambridge, Massachusetts 02138, USA

Note: This Paper is part of the APL Special Collection on Metastructures: From Physics to Applications.

^{a)} Author to whom correspondence should be addressed: zinlin@mit.edu

^{b)} Present address: NanoPhoton—Center for Nanophotonics, Technical University of Denmark, Ørstedes Plads 345A, DK-2800 Kgs. Lyngby, Denmark.

^{c)} Present address: Research Lab of Electronics, Massachusetts Institute of Technology, Cambridge, MA 02138, USA.

ABSTRACT

We present full-Maxwell topology-optimization design of a single-piece multilayer metalens, about 10 wavelengths λ in thickness, which simultaneously focuses over a 60° angular range and a 23% spectral bandwidth without suffering chromatic or angular aberration, a “plan-achromat.” At all angles and frequencies, it achieves diffraction-limited focusing (Strehl ratio >0.8) and an absolute focusing efficiency of $>50\%$. Both 2D and 3D axisymmetric designs are presented, optimized over $\sim 10^3$ degrees of freedom. We also demonstrate shortening the lens-to-sensor distance while producing the same image as for a longer “virtual” focal length and maintaining plan-achromaticity. These proof-of-concept designs demonstrate the ultra-compact multifunctionality that can be achieved by exploiting the full wave physics of subwavelength designs and motivate future work on design and fabrication of multilayer metaoptics.

Published under license by AIP Publishing. <https://doi.org/10.1063/5.0035419>

Modern augmented reality/virtual reality (AR/VR) applications demand increasingly sophisticated optical components with ultra-compact form-factors that can deliver the same level of performance as their conventional bulky counterparts. Metalenses and multilevel diffractive optics^{1–7} offer an innovative solution by replacing the bulky refractive components with much more compact interfaces, but they have not fundamentally altered the familiar multilens stacking strategy that uses ray optics to simultaneously minimize chromatic and off-axis aberrations [Fig. 1(a)]—a configuration that still consumes a large part of the device volume.^{8,9} We propose comprehensive nanophotonic solutions for miniaturization of optics, which reduce the role of ray mechanics and free-space propagation, by exploiting the much richer wave interactions occurring in nanostructured photonic media. Specifically, we present single-piece nanophotonic plan-achromats [Fig. 1(b)] for achromatic, aplanatic, and curvature-free focusing, that

is, realizing diffraction-limited focal spots [Strehl ratio (SR) >0.8 and absolute focusing efficiency (AE) of up to 65%] at precisely prescribed positions on a flat sensor over finite spectral and angular bandwidths. Our proposed solutions also allow for shortening the lens-to-sensor distance [Fig. 1(c)] by tailoring the output angles while maintaining the plan-achromaticity. Our primary goal in this work is to demonstrate the vast number of functionalities that can be incorporated into a small thickness ($\sim 10\lambda$, where λ is the operating wavelength) of low-index polymer structures by exploiting photonic inverse design,^{10–12} enabling over four orders of magnitude ($>10^4$) reduction in device thickness compared to traditional multilens systems. Rather than constraining our techniques to any specific fabrication method, our theoretical results reveal the untapped potential of single-piece 3D metaoptics, motivating future work to accelerate the advancement of nanoscale 3D fabrication technologies^{13–17} and computational

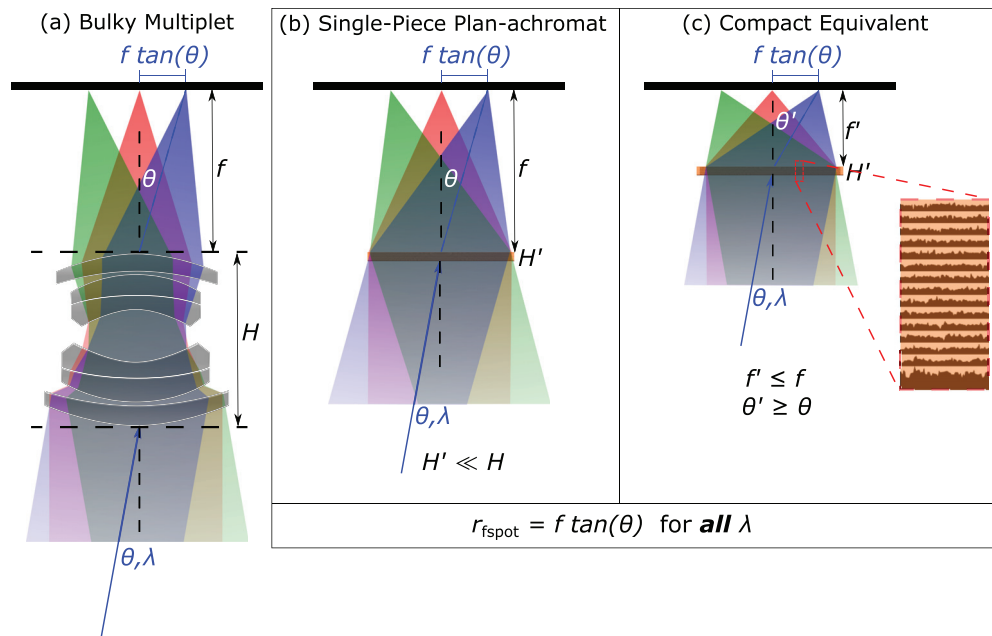


FIG. 1. (a) A bulky multiplet (an array of lenses) is needed to correct chromatic and geometric aberrations. (b) An ultra-compact nanophotonic single-piece plan-achromat can be inverse-designed to achieve both chromatic and geometric aberration corrections. (c) Further miniaturization is possible by designing a metastructure that can emulate a virtual focal distance $f < f'$ by stretching the out-going angles $\theta' > \theta$ while correcting the aberrations as well.

methods that will incorporate the evolving constraints of such technologies^{18–20} into 3D nanophotonic inverse design.

Previous work on metalens optics has been primarily devoted to achieving achromatic focusing at the normal incidence^{3,21,22} or correcting off-axis aberrations at a single frequency.^{6,7} In particular, a number of inverse design techniques have been explored to maximize metalens efficiencies over either spectral or angular bandwidths; such techniques involve combining locally periodic approximations, domain decomposition methods, or even full-wave Maxwell solvers with large-scale optimization algorithms^{10,12} to discover multifunctional metalens geometries.^{14,15,23–28} However, achieving single-piece plan-achromaticity (i.e., aberration-free focusing over simultaneous spectral and angular bandwidths) remains an open problem. While plan-achromaticity may be achieved by a multiplet metalens configuration,²⁹ such an approach still requires considerable propagation distance between individual lenses, which presents a significant hurdle to further reducing the device footprint. In contrast, our computational results indicate that it is possible to design single-piece unibody plan-achromats, enabled by utilizing 3D nanophotonics, thus circumventing the necessity of multiplet ray-optics designs.

In this work, we employ a topology-optimization³⁰ based inverse-design tool to design the metalenses. Topology optimization (TO) is a computational technique for inverse design that can handle extensive design spaces [$>10^9$ design variables (DVs)³¹] considering the dielectric permittivity at every spatial point as a DV.^{10–12} In contrast to heuristic search routines such as genetic algorithms³² or particle-swarm methods,³³ TO employs gradient-based optimization techniques to explore hundreds to billions of continuous DVs. Such a capability is made possible by a rapid computation of gradients (with respect to all the DVs) via adjoint methods,³⁴ which require just one

additional solution of Maxwell's equations^{10,12} in each design iteration. In fact, these techniques have been gaining traction lately in the field of photonic integrated circuits, especially for the design of compact modal multiplexers and converters.³⁵ More recently, TO-based inverse design methods have been extended to metasurfaces.^{15,23,24,26,27}

Here, we employ TO to design a single-piece nanophotonic plan-achromat, which focuses incoming plane waves at multiple frequencies and multiple angles. The focusing quality is measured by the Strehl ratio (SR); the SR above 0.8 is typically accepted as a gold standard for aberration-free imaging.² The SR is defined as

$$\text{SR} = \frac{P_{\text{peak}}}{P_{\text{airy}}}, \quad (1)$$

where P_{peak} is the peak intensity at the focal point and P_{airy} is the peak intensity of a diffraction-limited ideal airy disk normalized by the same transmitted power as that above the metalens. In particular, to design a plan-achromat, we maximize the minimum of SRs for multiple frequencies and angles $\{(\omega_i, \theta_i) : i = 1, \dots, N\}$; such a problem can be equivalently formulated in an epigraph form to obtain a differentiable optimization problem,³⁶ using an extra variable t ,

$$\max_{t, \varepsilon} t, \quad (2)$$

$$t \leq \text{SR}_i(\varepsilon), \quad i = 1, \dots, N. \quad (3)$$

In contrast to typical TO, where the relative permittivity $\varepsilon(\mathbf{r})$ is varied at each pixel, we consider varying the thickness profile of each layer¹⁵ with an aim to leverage the capabilities of 3D printing^{15,37} and thermal scanning probe lithography³⁸ for fabrication and characterization in future works.

In Fig. 2, we present a proof-of-concept 2D cylindrical lens design (invariant along y axis), which can focus 10 frequencies and 10 angles ($N = 100$) within a spectral and an angular bandwidth of 23% and 60° , respectively. The lens is 50λ wide and has a numerical aperture (NA) of 0.24; it consists of 20 layers of 3D-printable polymer (refractive index, ~ 1.5), corresponding to a total thickness of 12λ . Remarkably, TO discovers a design with a fairly uniform SR ≈ 0.89 , achieving aberration-free diffraction-limited focusing for all the design frequencies and angles; the uniformity is a typical by-product of the epigraph formulation.³⁶ In between the frequencies and angles targeted in the design process, the mean SR is >0.75 (Fig. 2, top-right inset). In addition to the SR, it is also instructive to compute the absolute focusing efficiency (AE), defined as the fraction of transmitted power within three full-widths at half-maximum (FWHM) around the focal peak divided by the total incident power. Figure 2 shows simulated AEs whose average is 55%; while the AE of our design may fall

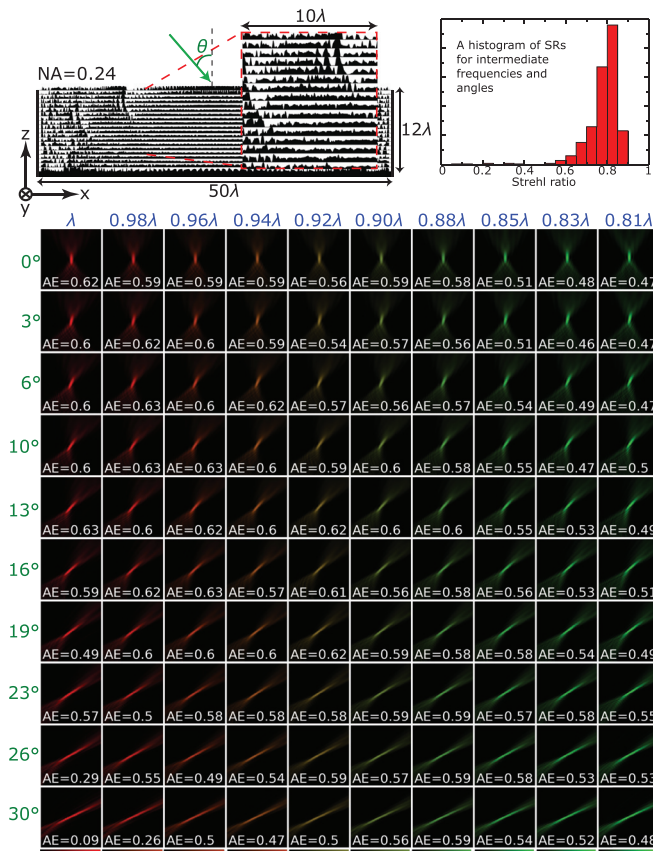


FIG. 2. A 2D cylindrical metalens (invariant along y) that corrects both chromatic and geometric aberrations within a spectral bandwidth of 23% and an angular bandwidth of 60° . The lens is 50λ wide and 12λ thick (note the scale bar) with a numerical aperture (NA) of 0.24; it is made up of 20 layers of 3D-printable polymer (refractive index = 1.5). The lens achieves a Strehl ratio (SR) above 0.8 (diffraction limited focusing) for each of the design frequencies and angles while exhibiting an averaged absolute focusing efficiency (AE) of 55%. The top-right inset shows a distribution of Strehl ratios within the designated spectral and angular bandwidths excluding the optimized frequencies and angles. Almost all SRs lie within 0.7 and 0.9 (mean SR >0.75); a few outliers correspond to edge frequencies and angles.

short of the efficiencies typically seen in bulky refractive lenses, it is better than or comparable to any previous achromatic metalens design,^{3,28} despite the multiple scatterings and complex interactions occurring within a multilayer geometry; further improvements in AE are likely possible if we also consider transmitted power as an additional constraint during optimization. The high SR implies that the 45% non-focused light is mainly lost to backscattering. Next, we demonstrate that our technique is not limited to small NA lenses; indeed, it can be straightforwardly scaled to higher NAs and larger lens widths. Figure 3 shows a wider and thicker design (125λ wide and 24λ thick) with a substantially higher NA of 0.7, achieving SR >0.85 for four frequencies and four angles with an average efficiency of 25%.

Having shown proof-of-concept 2D cylindrical lens designs, we now demonstrate that the proposed optimization framework can be used to design 3D plan-achromats. Designing a large-area fully free-form 3D plan-achromat would, however, demand much more intensive computational resources than were available to us in this work. A way to dramatically reduce the computational complexity is to exploit the axial symmetry (axisymmetry) of focusing.¹⁵ In other words, we restrict our 3D designs to be rotationally symmetric around a central axis. Doing this allows us to describe space using polar coordinates (r, ϕ, z) and exploit the ϕ -invariance $\varepsilon(r, \phi, z) = \varepsilon(r, z)$ (Fig. 4 top).

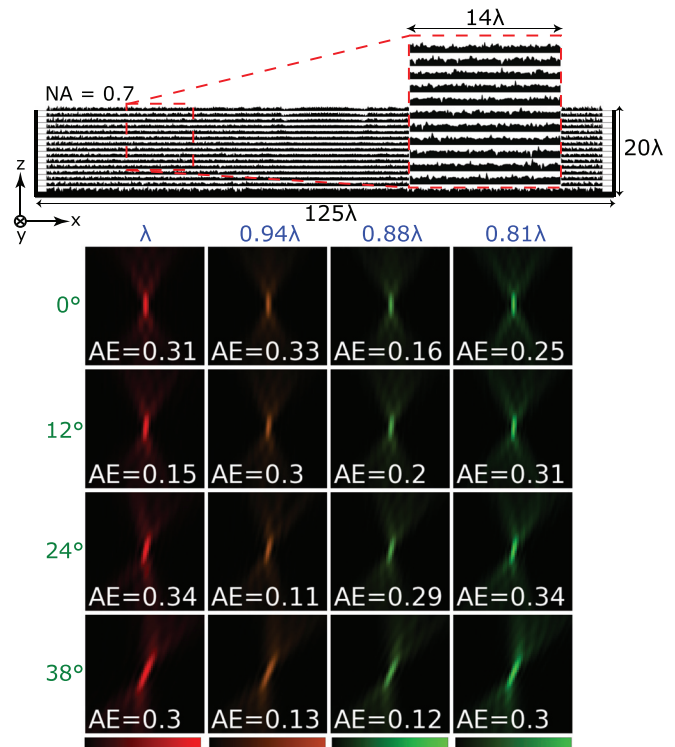


FIG. 3. A high-NA 2D cylindrical metalens that simultaneously corrects chromatic and geometric aberrations at four wavelengths and four angles within a spectral bandwidth of 23% and an angular bandwidth of 80° . The lens is 125λ wide and 24λ thick (note the scale bar) with an NA of 0.7; it is made up of 15 layers of 3D-printable polymer (refractive index = 1.5). The lens achieves an SR above 0.8 (diffraction limited focusing) for each of the design frequencies and angles while exhibiting an averaged absolute efficiency of 25%.

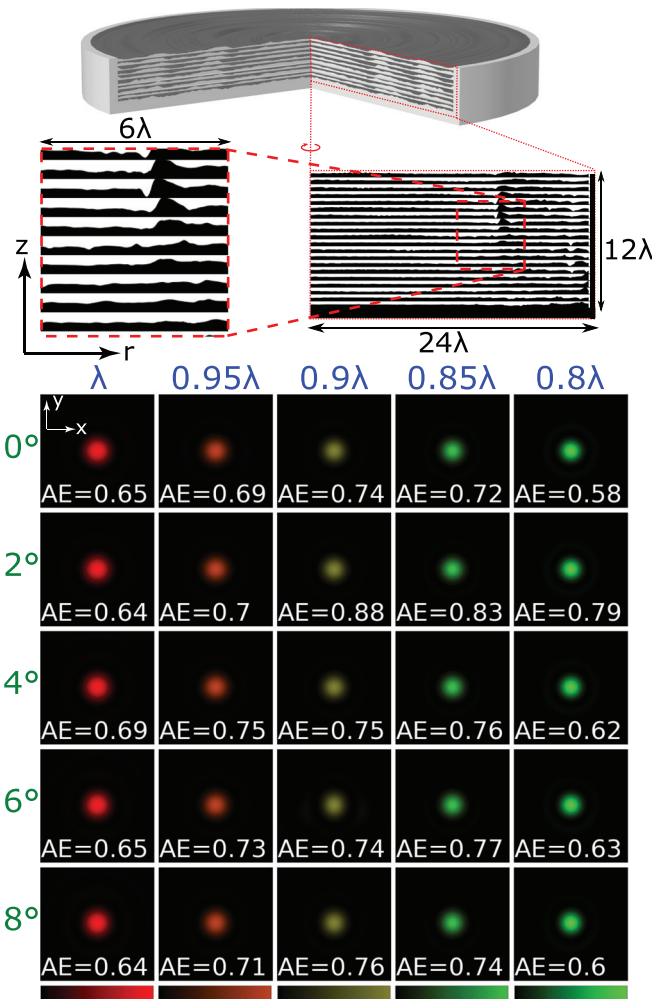


FIG. 4. An axisymmetric 3D metalens that simultaneously corrects chromatic and geometric aberrations at five wavelengths and five angles within a spectral bandwidth of 23% and an angular bandwidth of 16° . The lens has a diameter of 50λ wide and a thickness of 12λ (note the scale bar) with an NA of 0.12; it is made up of 20 layers of 3D-printable polymer (refractive index = 1.5). The lens achieves an SR above 0.8 (diffraction limited focusing) for each of the design frequencies and angles. The averaged absolute focusing efficiency (AE) is 71%.

This allows for the reduction of the 3D Maxwell equation to a set of independent 2D equations in (r, z) , each characterized by an integer angular momentum number m ,³⁹

$$\mathcal{D}^2 \mathbf{E}_m - \omega^2 \varepsilon(r, z) \mathbf{E}_m = i\omega \mathbf{J}_m, \quad (4)$$

where

$$\mathcal{D} = \begin{pmatrix} 0 & -\frac{\partial}{\partial z} & \frac{im}{r} \\ \frac{\partial}{\partial z} & 0 & -\frac{\partial}{\partial r} \\ -\frac{im}{r} & \frac{1}{r} \frac{\partial}{\partial r} & 0 \end{pmatrix}.$$

The total electric field \mathbf{E} is, then, given by the coherent sum of the individual fields times the exponential azimuthal factor ($\mathbf{E}_m e^{im\phi}$) over all m 's.

It is important to recognize that, in contrast to the axisymmetric material distribution ε , the incident current \mathbf{J} may not necessarily obey axisymmetry. For example, linearly polarized normally incident plane waves may be decomposed into two counter-rotating circularly polarized waves ($m = \pm 1$) both of which do obey axisymmetry. In contrast, any plane wave impinging on the lens at an oblique angle θ must be decomposed into an infinite number of axisymmetric components (with different m 's), the sum of which may be truncated at a finite number of terms, depending on the desired accuracy of the approximation; this decomposition (known as the Jacobi–Anger expansion) is given by

$$\mathbf{J} = A_x e^{ik_x x + ik_y y} \hat{\mathbf{x}} + A_y e^{ik_x x + ik_y y} \hat{\mathbf{y}}, \quad (5)$$

$$= \sum_m J_r^m e^{im\phi} \hat{\mathbf{r}} + \sum_m J_\phi^m e^{im\phi} \hat{\phi}, \quad (6)$$

$$\sqrt{k_x^2 + k_y^2} = \frac{2\pi}{\lambda} \sin \theta, \quad (7)$$

$$J_r^m = A_x P_m + A_y Q_m, \quad J_\phi^m = A_y P_m - A_x Q_m, \quad (8)$$

$$P_m(r) = \int_0^{2\pi} \exp [ik_x r \cos \phi + ik_y r \sin \phi - im\phi] \cos \phi d\phi, \quad (9)$$

$$Q_m(r) = \int_0^{2\pi} \exp [ik_x r \cos \phi + ik_y r \sin \phi - im\phi] \sin \phi d\phi, \quad (10)$$

where the integrals P and Q can be evaluated by Bessel's functions. Therefore, the total electric field response of an axisymmetric lens under off-axis plane wave incidence is a coherent sum of individual fields in response to the current components \mathbf{J}_m , which can be computed in a highly parallel fashion.

We combine the axisymmetric Maxwell solver with topology optimization to design a fully 3D single-piece plan-achromat (Fig. 4), rigorously taking into account off-axis angular aberrations. The lens has a diameter of 50λ and a thickness of 12λ with an NA of 0.12. It is optimized for aberration-free focusing at five frequencies and five angles ($N=25$) within 23% bandwidth and 16° field of view. The lens achieves diffraction-limited focusing with $\text{SR} > 0.86$ for all the design frequencies and angles, while the average absolute efficiency is 72%. To accurately model the off-axis angles, we consider up to 50 angular mode numbers so that the truncation error is less than 1% [compare Eqs. (5) and (6)], distributing our simulations over ~ 1000 CPUs with a computational time of about a week. Much larger diameters and numerical apertures can be designed by combining our approach with an overlapping domain method.²⁷

While we have shown that it is possible to dramatically reduce a cm-scale multiplet plan-achromat to a micrometer-scale single-piece with nanoscale 3D structuring, the overall system may still remain undesirably bulky because of the free space between the lens and the sensor.⁴⁰ We note that to further reduce this distance is not a simple matter of just designing a lens with a shorter focal length because conventional ray optics dictates that in order to achieve a desired magnification at a finite sensor resolution, the lens and sensor must be sufficiently separated. Conventionally, “compact imitations” such as a telephoto array are used to mimic the effect of a long-focus lens within a physically shorter device. On the other hand, it should be clear that

the actual distance between the optical component and the sensor should not matter as long as the sensor measures the same output for any given input in the compact imitation as in the long-focus original. Since an arbitrary input can be decomposed into a sum of plane waves, the compact imitation must reproduce, for each input angle θ , a corresponding focal spot at the same position on a near sensor as the original would produce on a far sensor, i.e., the focal spot for θ must be formed at $f \tan \theta$ away from the sensor center where f is the virtual focal length of a desired long-focus lens, which may be longer than the actual lens-sensor distance $f' > f$ in the compact equivalent [Fig. 5 (top left inset) and also Fig. 1(c)]. This effectively means that any nanostructured equivalent, which labors to shorten the lens-sensor distance, must stretch the output angle as specified by the relation $\theta' = \tan^{-1}\left(\frac{f}{f'} \tan \theta\right)$. (Optical etendue is conserved because the stretched angular output is compensated by a reduced numerical aperture that is smaller than what is implied by the physical width and lens-to-sensor distance.) Our inverse design formulation is naturally

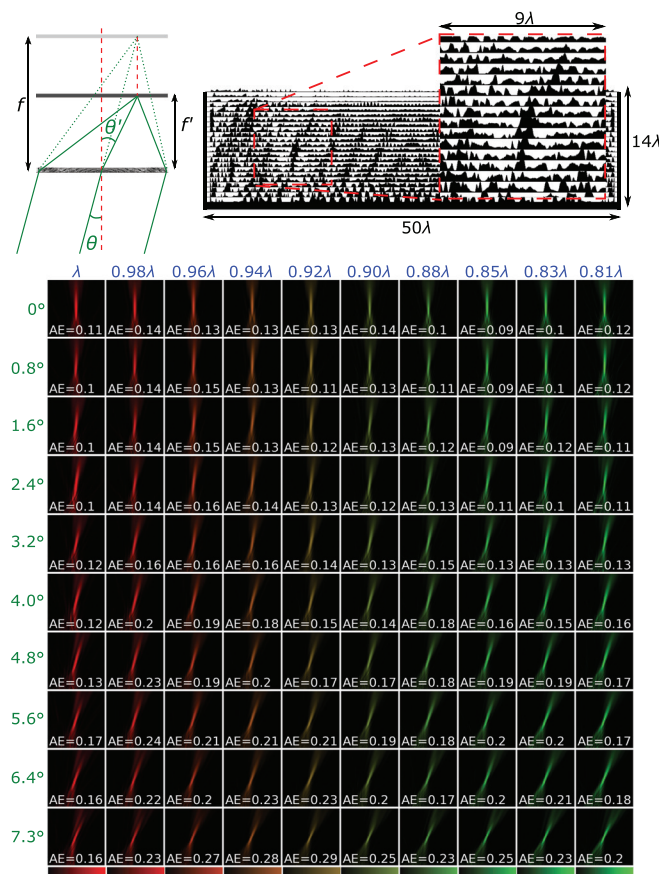


FIG. 5. A 2D cylindrical metalens that emulates a virtual focal length of 200λ (54% compression of lens-to-sensor distance) while simultaneously correcting chromatic and geometric aberrations at 10 wavelengths and 10 angles within a spectral bandwidth of 23% and an angular bandwidth of 16° . The lens has a diameter of 50λ wide and a thickness of 12λ thick (note the scale bar) with a virtual NA of 0.12; it is made up of 23 layers of 3D-printable polymer (refractive index = 1.5). The lens achieves an SR above 0.8 (diffraction limited focusing) for each of the design frequencies and angles.

suiting to design for such effects because we can explicitly specify an arbitrary input-output relation to our device.⁴¹ Here, we note that recently, an alternative approach to squeezing free space has also been proposed based on non-local metamaterials;^{40,42} in contrast, our approach specifically considers the space-squeezing problem in an integral fashion, simultaneously with the focusing problem, and seeks to discover an “all-in-one unibody” nanophotonic space-squeezing plan-achromat.

Figure 5 shows a proof-of-concept 2D plan-achromat space-squeezer with a virtual focal length of 200λ but a physical lens-to-sensor distance of 130λ (54% compression). The lens is 50λ wide and 12λ thick, with a virtual NA of 0.12, and is optimized to perform at 10 frequencies and 10 angles over spectral and angular bandwidths of 23% and 16° , respectively, achieving virtual SR > 0.8 for all the design frequencies and angles (note that the virtual SR is defined relative to the virtual airy disk, i.e., the ideal airy disk that would have been formed at the virtual focal distance of 200λ). One trade-off we found in the space-squeezer design is that the bigger the compression, the smaller the absolute focusing efficiency even for a small numerical aperture. While additional optimization constraints may be used to improve the transmission efficiency, we speculate that there exists a fundamental trade-off between compression and transmission—a theoretical question we will seek to elucidate in future work. On the other hand, such a trade-off may be entirely circumvented in an end-to-end framework, in which a front-end photonic design is fully coupled with a back-end computational reconstruction algorithm.⁴³

In summary, we have presented computational designs for single-piece plan achromats with SR > 0.8 and focusing efficiencies up to 65%. We have also demonstrated that by solving the Maxwell equations under axial symmetry, one can design 3D axisymmetric plan-achromats that fully consider off-axis propagation. Our solutions also suggest the possibility of further reducing the lens-to-sensor distance by manipulating the relation between input and output angles and mimicking a longer virtual focal length.

Our optimizations were performed over ~ 1000 CPUs within one day to a week. We surmise that it is possible to design high-NA single-piece plan-achromats with millimeters in diameter and $\sim 100 \mu\text{m}$ in thickness, given sufficient computational resources on the order of ~ 3000 CPUs combined with advanced numerical solvers, which exploits the overlapping domains technique.²⁷

Our theoretical results demonstrate the untapped potential of volumetric nanophotonics and set the foundations for future works, which will be devoted to developing 3D devices tailored for specific fabrication technologies. For any given fabrication technology, there are a wealth of computational techniques to impose corresponding design constraints on feature sizes,²⁰ connectivity,¹⁹ and mechanical stability.¹⁸ For our proof-of-concept designs in this paper, it was convenient to parameterize the structures in terms of variable-height layers, but this is merely an artifact of this parameterization and is not fundamental to plan-achromat functionality. We expect that any degradation in performance arising from imposing fabrication constraints may be offset by increasing the device volumes (optimizing over even larger design spaces). Furthermore, broadband devices tend to be inherently robust to small manufacturing defects,⁴⁴ but standard techniques are available to incorporate additional robustness into TO if needed.¹⁰

Experimentally, there has been a surge of interest in fabricating multilayer metaoptics devices.^{45,46} These designs require fabrication techniques more advanced than traditional CMOS single-step lithography, such as multistep lithography or laser writing techniques. Recent works suggest that 3D nanofabrication is poised to enable enhanced capabilities in 3D nanophotonics such as 3D interconnects,¹⁶ fiber couplers,¹⁷ and metasurfaces.^{14,15} A particularly promising platform for volumetric metaoptics is the recently demonstrated implosion fabrication technique,¹³ which has the potential for realizing relatively constraint-free 3D geometries (such as multimaterial high-index structures held in place by a low-index background matrix) with feature sizes as small as a few tens of nanometers. Our work motivates further efforts to take advantage of emerging advances in 3D fabrication by demonstrating the potential of inverse-designed 3D metaoptics.

We note that our results represent an all-optical solution to imaging that does not require extensive calibration measurements. An alternative strategy that can ease the burden on optics is to measure “imperfect” point-spread functions and apply image processing algorithms to extract a faithful image.⁴⁷ Recently, we have also shown that nanophotonic structures can be inverse-designed in a holistic end-to-end fashion together with any image processing backend.⁴³ Ultimately, we expect that an optimal mix of hardware and software can be found to solve the most challenging problems in modern optical technologies and to pave the way for extraordinary functionalities that have not yet been explored.

We thank John Joannopoulos for helpful discussion. This work was supported in part by Villum Fonden through the NATEC (Nanophotonics for Tera-bit Communications) Centre (Grant No. 8692), the Danish National Research Foundation through NanoPhoton Center for Nanophotonics (Grant No. DNRF147), the U.S. Army Research Office through the Institute for Soldier Nanotechnologies (Award No. W911NF-18-2-0048), and the MIT-IBM Watson AI Laboratory (Challenge No. 2415).

DATA AVAILABILITY

The data that support the findings of this study are available from the corresponding author upon reasonable request.

REFERENCES

- N. Yu and F. Capasso, “Flat optics with designer metasurfaces,” *Nat. Mater.* **13**, 139 (2014).
- M. Khorasaninejad, W. T. Chen, R. C. Devlin, J. Oh, A. Y. Zhu, and F. Capasso, “Metalenses at visible wavelengths: Diffraction-limited focusing and subwavelength resolution imaging,” *Science* **352**, 1190–1194 (2016).
- W. T. Chen, A. Y. Zhu, V. Sanjeev, M. Khorasaninejad, Z. Shi, E. Lee, and F. Capasso, “A broadband achromatic metalens for focusing and imaging in the visible,” *Nat. Nanotechnol.* **13**, 220 (2018).
- G. Kim, J. A. Domínguez-Caballero, and R. Menon, “Design and analysis of multi-wavelength diffractive optics,” *Opt. Express* **20**, 2814–2823 (2012).
- M. Meem, S. Banerji, C. Pies, T. Oberbiermann, A. Majumder, B. Sensale-Rodriguez, and R. Menon, “Large-area, high-numerical-aperture multi-level diffractive lens via inverse design,” *Optica* **7**, 252–253 (2020).
- A. Arbabi, E. Arbabi, S. M. Kamali, Y. Horie, S. Han, and A. Faraon, “Miniature optical planar camera based on a wide-angle metasurface doublet corrected for monochromatic aberrations,” *Nat. Commun.* **7**, 13682 (2016).
- B. Groever, W. T. Chen, and F. Capasso, “Meta-lens doublet in the visible region,” *Nano Lett.* **17**, 4902–4907 (2017).
- B. C. Kress and W. J. Cummings, “11-1: Invited paper: Towards the ultimate mixed reality experience: Hologram display architecture choices,” in *SID Symposium Digest of Technical Papers* (Wiley Online Library, 2017), Vol. 48, pp. 127–131.
- B. C. Kress, “Digital optical elements and technologies (EDO19): Applications to AR/VR/MR,” in *Digital Optical Technologies 2019* (International Society for Optics and Photonics, 2019), Vol. 11062, p. 1106222.
- J. S. Jensen and O. Sigmund, “Topology optimization for nano-photonics,” *Laser Photonics Rev.* **5**, 308–321 (2011).
- C. M. Lalau-Keraly, S. Bhargava, O. D. Miller, and E. Yablonovitch, “Adjoint shape optimization applied to electromagnetic design,” *Opt. Express* **21**, 21693–21701 (2013).
- S. Molesky, Z. Lin, A. Y. Piggott, W. Jin, J. Vucković, and A. W. Rodriguez, “Inverse design in nanophotonics,” *Nat. Photonics* **12**, 659 (2018).
- D. Oran, S. G. Rodrigues, R. Gao, S. Asano, M. A. Skylar-Scott, F. Chen, P. W. Tillberg, A. H. Marblestone, and E. S. Boyden, “3D nanofabrication by volumetric deposition and controlled shrinkage of patterned scaffolds,” *Science* **362**, 1281–1285 (2018).
- A. Zhan, R. Gibson, J. Whitehead, E. Smith, J. R. Hendrickson, and A. Majumdar, “Controlling three-dimensional optical fields via inverse Mie scattering,” *Sci. Adv.* **5**, eaax4769 (2019).
- R. E. Christiansen, Z. Lin, C. Roques-Carmes, Y. Salamin, S. E. Kooi, J. D. Joannopoulos, M. Soljačić, and S. G. Johnson, “Fullwave maxwell inverse design of axisymmetric, tunable, and multi-scale multi-wavelength metalenses,” *Opt. Express* **28**, 33854–33868 (2020).
- J. Moughames, X. Porte, M. Thiel, G. Ulliac, L. Larger, M. Jacquot, M. Kadic, and D. Brunner, “Three-dimensional waveguide interconnects for scalable integration of photonic neural networks,” *Optica* **7**, 640–646 (2020).
- H. Gehring, M. Blaicher, W. Hartmann, P. Varytis, K. Busch, M. Wegener, and W. Pernice, “Low-loss fiber-to-chip couplers with ultrawide optical bandwidth,” *APL Photonics* **4**, 010801 (2019).
- Y. Augenstein and C. Rockstuhl, “Inverse design of nanophotonic devices with structural integrity,” *ACS Photonics* **7**, 2190–2196 (2020).
- Q. Li, C. Wenjiang, L. Shutian, and L. Tong, “Structural topology optimization considering connectivity constraint,” *Struct. Multidiscip. Optim.* **54**, 971–984 (2016).
- M. Zhou, B. S. Lazarov, F. Wang, and O. Sigmund, “Minimum length scale in topology optimization by geometric constraints,” *Comput. Methods Appl. Mech. Eng.* **293**, 266–282 (2015).
- S. Wang, P. C. Wu, V.-C. Su, Y.-C. Lai, M.-K. Chen, H. Y. Kuo, B. H. Chen, Y. H. Chen, T.-T. Huang, J.-H. Wang *et al.*, “A broadband achromatic metalens in the visible,” *Nat. Nanotechnol.* **13**, 227 (2018).
- S. Shrestha, A. C. Overvig, M. Lu, A. Stein, and N. Yu, “Broadband achromatic dielectric metalenses,” *Light* **7**, 85 (2018).
- D. Sell, J. Yang, S. Doshay, R. Yang, and J. A. Fan, “Large-angle, multifunctional metagratings based on freeform multimode geometries,” *Nano Lett.* **17**, 3752–3757 (2017).
- Z. Lin, B. Groever, F. Capasso, A. W. Rodriguez, and M. Lončar, “Topology-optimized multilayered metaoptics,” *Phys. Rev. Appl.* **9**, 044030 (2018).
- R. Pestourie, C. Pérez-Arancibia, Z. Lin, W. Shin, F. Capasso, and S. G. Johnson, “Inverse design of large-area metasurfaces,” *Opt. Express* **26**, 33732–33747 (2018).
- Z. Lin, V. Liu, R. Pestourie, and S. G. Johnson, “Topology optimization of freeform large-area metasurfaces,” *Opt. Express* **27**, 15765–15775 (2019).
- Z. Lin and S. G. Johnson, “Overlapping domains for topology optimization of large-area metasurfaces,” *Opt. Express* **27**, 32445–32453 (2019).
- H. Chung and O. D. Miller, “High-NA achromatic metalenses by inverse design,” *Opt. Express* **28**, 6945–6965 (2020).
- S. Shrestha, A. Overvig, and N. Yu, “Multi-element meta-lens systems for imaging,” in *2019 Conference on Lasers and Electro-Optics (CLEO) (IEEE, 2019)*, pp. 1–2.
- M. P. Bendsoe and O. Sigmund, *Topology Optimization: Theory, Methods, and Applications* (Springer Science & Business Media, 2013).
- N. Aage, E. Andreassen, B. S. Lazarov, and O. Sigmund, “Giga-voxel computational morphogenesis for structural design,” *Nature* **550**, 84–86 (2017).
- M. Mitchell, *An Introduction to Genetic Algorithms* (MIT Press, 1998).

- ³³J. Kennedy, "Particle swarm optimization," *Encyclopedia of Machine Learning* (Springer, 2011), pp. 760–766.
- ³⁴G. Strang, *Computational Science and Engineering* (Wellesley-Cambridge Press, Wellesley, 2007), Vol. 791.
- ³⁵A. Y. Piggott, J. Lu, K. G. Lagoudakis, J. Petykiewicz, T. M. Babinec, and J. Vučković, "Inverse design and demonstration of a compact and broadband on-chip wavelength demultiplexer," *Nat. Photonics* **9**, 374–377 (2015).
- ³⁶S. Boyd, S. P. Boyd, and L. Vandenberghe, *Convex Optimization* (Cambridge University Press, 2004).
- ³⁷T. Gissibl, S. Thiele, A. Herkommer, and H. Giessen, "Two-photon direct laser writing of ultracompact multi-lens objectives," *Nat. Photonics* **10**, 554–560 (2016).
- ³⁸N. Lassaline, R. Brechbühler, S. J. Vonk, K. Ridderbeek, M. Spieser, S. Bisig, B. Le Feber, F. T. Rabouw, and D. J. Norris, "Optical Fourier surfaces," *Nature* **582**, 506–510 (2020).
- ³⁹A. Taflove and S. C. Hagness, *Computational Electrodynamics: The Finite-Difference Time-Domain Method* (Artech House, 2005).
- ⁴⁰O. Reshef, M. P. DelMastro, K. K. Bearne, A. H. Alhulaymi, L. Giner, R. W. Boyd, and J. S. Lundeen, "Towards ultra-thin imaging systems: An optic that replaces space," [arXiv:2002.06791](https://arxiv.org/abs/2002.06791) (2020).
- ⁴¹R. E. Christiansen and O. Sigmund, "Designing meta material slabs exhibiting negative refraction using topology optimization," *Struct. Multidiscip. Optim.* **54**, 469–482 (2016).
- ⁴²C. Guo, H. Wang, and S. Fan, "Squeeze free space with nonlocal flat optics," [arXiv:2003.06918](https://arxiv.org/abs/2003.06918) (2020).
- ⁴³Z. Lin, C. Roques-Carmes, R. Pestourie, M. Soljačić, A. Majumdar, and S. G. Johnson, "End-to-end nanophotonic inverse design for imaging and polarimetry," *Nanophotonics* **1**, 20200579 (2020).
- ⁴⁴A. Oskooi, A. Mutapcic, S. Noda, J. D. Joannopoulos, S. P. Boyd, and S. G. Johnson, "Robust optimization of adiabatic tapers for coupling to slow-light photonic-crystal waveguides," *Opt. Express* **20**, 21558–21575 (2012).
- ⁴⁵M. Mansouree, H. Kwon, E. Arbabi, A. McClung, A. Faraon, and A. Arbabi, "Multifunctional 2.5D metastructures enabled by adjoint optimization," *Optica* **7**, 77–84 (2020).
- ⁴⁶Y. Zhou, I. I. Kravchenko, H. Wang, J. R. Nolen, G. Gu, and J. Valentine, "Multilayer noninteracting dielectric metasurfaces for multiwavelength meta-optics," *Nano Lett.* **18**, 7529–7537 (2018).
- ⁴⁷A. Tarantola, *Inverse Problem Theory and Methods for Model Parameter Estimation* (SIAM, 2005).